Supporting Information for

$CdF(C_6H_4NO_2)(H_2O)$: A UV Nonlinear Optical Material with Unprecedented SHG and Birefringence via a π-Conjugated Rings and Unique "Warren Truss Structure"

Jie Gou, †[a,b] Yaolong Zhu, †[a] Xin Su, [b] Can Yang, [a] Yunjie Wang, [b] Qingwen Zhu,[a] Yi Xiong, [a] and Qi Wu*[a]

[a] Jie Gou, Yaolong Zhu, Can Yang, Qingwen Zhu, Yi Xiong, and Qi Wu,
State Key Laboratory of New Textile Materials and Advanced Processing Technologies, Wuhan Textile University, Wuhan 430200, People's Republic of China, E-mail: wuqi2011@whu.edu.cn;

[b] J. Gou, Xin. Su, YunJie Wang,
Xinjiang Laboratory of Phase Transitions and Microstructures in Condensed Matter Physics, College of Physical Science and Technology. yili-Normal University yi ning, 835000, China.

†These authors contributed equally.

Contents

Experimental Procedures

Reagents

Cadmium fluoride (CdF_2, 99%, Adamas), Methyl nicotinate ($C_7H_7NO_2$, 99%, Adamas). They are all used without further purification.

Synthesis

The compound $CdF(C_6H_4NO_2)(H_2O)$ was synthesized by hydrothermal. $C_7H_7NO_2$ (0.274 g, 2 mmol), CdF_2 (0.3 g, 2 mmol) and H_2O (3 mL) were added to the reaction kettle, the reaction kettle was warmed from room temperature 30 °C to 120 °C after 2 h. The reaction kettle was kept at 120 °C for 3 days and then cooled down for 2 days to 30 °C slowly at 3 °C/h to obtain white bulk crystals.

Instruments and Property Characterizations

Single Crystal X-ray Diffraction

The single-crystal *X*-ray diffraction (XRD) data for $CdF(C_6H_4NO_2)(H_2O)$ were collected on an XtaLAB Synergy R equipped with a graphite monochromator using Mo Kα radiation (λ = 0.71073 Å) at 298 K. The crystal structure was solved by Direct Methods with Olex2 and refined by least-squares techniques on F^2 with anisotropic thermal parameters for all atoms.[1] Atomic coordinates, equivalent isotropic displacement parameters, bond valence sum (BVS), selected bond lengths and angles, and hydrogen bond distances are listed in Tables S1 - S6.

Powder X-ray Diffraction

Powder *X*-ray diffraction data were recorded on an Advance diffractometer at A temperature of 40 kV, 100 mA, Cu Kα1 radiation (Bruker D8, radiation wave number 1.5406 Å), scanning speed of 10 °/min, and scanning Angle range of 10-70°. The phase purity was determined by powder *X*-ray diffraction.

Infrared (IR) Spectrum

The IR spectra was collected on a Nicolet iS5 Fourier-transformed infrared (FTIR) spectrometer at room temperature (4000-400 cm^{-1}). The sample and dry KBr are mixed and ground in a certain proportion and pressed into flakes for measurement. (weight ratio = 1:100).

UV-vis Diffuse Reflectance Spectroscopy

The UV-vis diffuse reflectance spectra were obtained by using a Varian Cary 5000 spectrophotometer with a scan range of 200-800 nm at room temperature. The spectrally pure barium sulfate was selected as a reference (100% reflectance), and a ground powder sample was coated on its surface for testing.

Thermogravimetric (TG) Analysis

Thermogravimetric analysis (TGA) was carried out using a Netzsch STA 449 F5 analyzer. The specific method is to weigh a sample of about 6 mg and place it in a platinum crucible, heat it from room temperature to 800 ^{o}C at a rate of 10 K min^{-1} in a N_2 gas atmosphere.

***X*-ray Photoelectron Spectroscopy**

X-ray photoelectron spectroscopy (XPS) measurement was performed with a AXIS SUPRA+ spectrophotometer.

Second Harmonic Generation (SHG) Measurement

The second-order NLO measurements of the powder samples were performed at room temperature, and the SHG effect of the powder samples was measured using a Q-switched 1064 nm Nd: YAG laser by using the improved Kurtz and Perry methods. Polycrystalline samples of this compound were sieved into different particle sizes (35-50, 50-74, 74-100, 100-154, 154-180, 180-280 and 280-450 μm) to investigate whether its SHG response could be phase matched. The reference substance KH_2PO_4 (KDP) was selected to compare with the SHG efficiency of the sample, so as to evaluate the second-order NLO effect of the measured sample.

Birefringence Measurements

The birefringence of crystalline $CdF(C_6H_4NO_2)(H_2O)$ was assessed with a polarizing microscope (ZEISS Axioscope A1) equipped with a Berek compensator. The wavelength of the light source was 546 nm. The birefringence were calculated according to the following equation: ΔR (retardation) = $|N_s - N_f| \times T = \Delta n \times T$ where ΔR denotes the optical path difference, Δn represents the birefringence, and T is the thickness of the crystal.[2] The positive and negative rotation of compensation affords the relative retardation. The clear boundaries between the first, second, and third-order interference colors result in a small relative error. To improve the accuracy of the

birefringence, transparent regular plate-like $CdF(C_6H_4NO_2)(H_2O)$ crystals were chosen for the measurements.

Computational Methods

The first-principle calculation of $CdF(C_6H_4NO_2)(H_2O)$ is based on the CASTEP module of Materials Studio software package, and the geometric structure optimization of the system is carried out by density functional theory.[3] The exchange correlation functional is described by the generalized gradient approximation GGA-PBE.[4] the truncation energy is set to 940 eV, and the Monkhorst-Pack[5] *k* point grid 3 × 6 × 2 is selected in the first Brillouin region to ensure the accuracy of the calculation results. Self-consistent iterative convergence (SCF) is 5.0×10^{-7} eV $atom^{-1}$, the maximum displacement convergence is 5.0×10^{-4} Å, the internal stress is 0.02 GPa, the force on the atom is 0.01 eV A^{-1}, and the energy convergence is within 5.0×10^{-6} eV $atom^{-1}$. The ion-electron interactions of all atoms are modeled by the ultra-soft pseudopotential, and the atomic electron configurations are C($2s^22p^2$), H($1s^1$), N($2s^22p^3$), O($2s^22p^4$), Cd($5s^24d^{10}$), F($2s^22p^5$). The SHG coefficients d_{ij} were calculated through the "velocity-gauge" formula.[6, 7]

Results and Discussion

Table S1. Crystal data and structure refinement for $CdF(C_6H_4NO_2)(H_2O)$.

Compound	**$CdF(C_6H_4NO_2)(H_2O)$**
Formula weight	271.52
Temperature (K)	296.15
Crystal system	monoclinic
Space group	$P2_1$
a (Å)	9.2128 (13)
b (Å)	4.2589 (7)
c (Å)	10.7400 (17)
α (Å)	90
β (Å)	114.506(4)
γ (Å)	90
Volume (Å^3)	383.44 (10)
Z	2
ρ_{calc} (g/cm^3)	2.352
μ (mm^{-1})	2.828
F (000)	260
2θ range for data collection/°	7.606 to 52.754
Data/restraint/parameters	1574/1/111
GOF on F^2	1.128
R, wR [I≥2σ (I)]	R_1 = 0.0196, wR_2 = 0.0522
R, wR [all data]	R_1 = 0.0202, wR_2 = 0.0524
Largest diff. peak/hole (e Å^{-3})	1.19/-0.47
Flack parameter	0.11(6)

$R_1 = F_0 - F_0/F_0$ and $wR^2 = [w (F_0{}^2 - F_0{}^2)^2 / wF_0{}^4]$

Table S2. Fractional Atomic Coordinates ($\times 10^4$) and Equivalent Isotropic Displacement Parameters ($Å^2 \times 10^3$) for $CdF(C_6H_4NO_2)(H_2O)$. U_{eq} is defined as 1/3 of of the trace of the orthogonalised U_{ij} tensor.

Atom	*x*	*y*	*z*	*U*(eq)	BVS
Cd1	9022.9(2)	4708.0(16)	5740.7(2)	19.45(12)	2.06
F1	9490(3)	-280(17)	5542(2)	29.2(5)	0.95
O1	6651(3)	5259(11)	2120(3)	31.0(11)	1.36
O3	6538(4)	4850(30)	4155(3)	40.2(10)	1.72
O2	11379(4)	5241(13)	7661(4)	31.0(13)	1.79
C3	3726(6)	8541(14)	1053(5)	30.3(12)	4.64
C2	2285(5)	10100(20)	625(5)	34.7(14)	4.72
N1	2169(5)	9111(13)	2767(4)	25.5(15)	3.20
C4	4398(5)	7302(13)	2362(5)	24.7(10)	4.12
C5	3585(5)	7644(13)	3190(5)	24.9(10)	4.49
C1	1540(5)	10282(15)	1490(5)	30.4(17)	4.58
C6	5993(5)	5668(12)	2917(5)	26.17(11)	3.38

Table S3. Anisotropic Displacement Parameters ($Å^2 \times 10^3$) for $CdF(C_6H_4NO_2)(H_2O)$. The Anisotropic displacement factor exponent takes the form: $-2\pi^2$[h2a*2U_{11}+2hka*b*U_{12}+…].

Atom	U_{11}	U_{22}	U_{33}	U_{23}	U_{13}	U_{12}
Cd1	21.3(3)	16.4(3)	23.0(3)	0.4(3)	13.4(2)	0.0(3)
F1	39(2)	16.2(18)	42(2)	2(4)	28.4(18)	1(4)
O1	26(2)	37(5)	32(3)	2(3)	16(2)	6(3)
O3	22(2)	56(5)	31(3)	9(5)	11.4(19)	-1(5)
O2	37(2)	54(7)	44(3)	5(3)	14(2)	5(3)
C3	32(4)	39(5)	24(4)	0(3)	11(3)	-1(3)
C2	33(3)	43(7)	24(3)	8(5)	12(3)	3(5)
N1	24(3)	29(7)	27(3)	5(3)	14(2)	8(3)
C4	20(3)	32(4)	24(3)	-2(3)	11(3)	-1(3)
C5	22(3)	32(4)	19(4)	5(3)	12(3)	7(3)
C1	28(3)	39(8)	24(4)	11(4)	9(3)	17(4)
C6	18(3)	26(4)	34(4)	-2(3)	12(3)	-3(3)

Table S4. Bond Lengths (Å) for $CdF(C_6H_4NO_2)(H_2O)$.

Bond	Lengths (Å)	Bond	Lengths (Å)
Cd1-F1	2.195(7)	C3-C2	1.381(7)
Cd1-F1[1]	2.311(2)	C3-C4	1.384(7)
Cd1-F1[2]	2.205(7)	C2-C1	1.367(7)
Cd1-O3	2.216(3)	N1-C5	1.344(7)
Cd1-O2	2.303(3)	N1-C1	1.344(6)
Cd1-N1[3]	2.302(4)	C4-C5	1.387(7)
O1-C6	1.249(6)	C4-C6	1.507(6)
O3-C6	1.260(6)		

[1]2-*X*, 1/2+*Y*, 1-*Z*; [2]+*X*, 1+*Y*, +*Z*; [3]1-*X*, -1/2+*Y*, 1-*Z*

Table S5. Bond Angles for $CdF(C_6H_4NO_2)(H_2O)$.

Bond	Angles (°)	Bond	Angles (°)
F1-Cd1-F1[1]	150.82(12)	Cd1[4]-F1-Cd1[5]	104.1(2)
F1-Cd1-F1[2]	75.86(15)	Cd1-F1-Cd1[5]	104.4(2)
F1[1]-Cd1-F1[2]	75.67(15)	C6-O3-Cd1	130.7(3)
F1[1]-Cd1-O3	94.5(3)	C2-C3-C4	119.0(5)
F1-Cd1-O3	97.7(3)	C1-C2-C3	119.1(5)
F1-Cd1-O2	91.86(15)	C5-N1-Cd1[6]	119.5(3)
F1[1]-Cd1-O2	80.96(16)	C5-N1-C1	117.7(4)
F1[1]-Cd1-N1[3]	110.05(17)	C1-N1-Cd1[6]	122.7(3)
F1[1]-Cd1-N1[3]	97.48(17)	C3-C4-C5	118.5(5)
O3-Cd1-F1[2]	102.74(11)	C3-C4-C6	122.0(4)
O3-Cd1-O2	167.2(2)	C5-C4-C6	119.5(4)
O3-Cd1-N1[3]	84.21(14)	N1-C5-C4	122.6(4)
O1-Cd1-F1[2]	87.82(11)	N1-C1-C2	123.1(5)
N1[3]-Cd1-F1[2]	170.85(19)	O1-C6-O3	126.2(5)
N1[3]-Cd1-O2	86.12(14)	O1-C6-C4	117.7(4)
Cd-F1-Cd1[4]	150.83(12)	O3-C6-C4	116.1(5)

[1]+*X*, 1+*Y*, +*Z*; [2]2-*X*, 1/2+*Y*, 1-*Z*; [3]1-*X*, 1/2+*Y*, 1-*Z*; [4]+*X*, -1+*Y*, +*Z*; [5]2-*X*, -1/2+*Y*, 1-*Z*; [6]1-*X*, 1/2+*Y*, 1-*Z*

Table S6. Hydrogen Bonds for $CdF(C_6H_4NO_2)(H_2O)$.

D-H…A	**d_{D-H} (Å)**	**d_{H-A} (Å)**	**D_{D-A} (Å)**	**D-H-A (°)**
O2-H2A…O1	0.85	1.90	2.738(6)	167
O2-H2B…O1	0.85	1.95	2.750(7)	157
C1-H1…O2	0.93	2.59	3.178(7)	121
C5-H5…O3	0.93	2.42	2.748(8)	101
C5-H5…O3	0.93	2.53	3.049(7)	116

Table S7. Calculated dipole moment components of $CdF(C_6H_4NO_2)(H_2O)$.

Dipole moment (au)			
	x	*y*	*z*
electronic	-2059.316364	-1182.283561	1697.312777
nuclear	2059.377874	1182.847437	1699.662590
net	0.061509	0.277172	2.349812
Dipole magnitude	2.41730 au		6.1442 debye

Table S8. Comparison of the performance of $CdF(C_6H_4NO_2)(H_2O)$ with other metal fluorides.

Compounds	**Cutoff**	**SHG**	**Δ*n***	**[Ref.]**
$BaMgF_4$	125	0.085	0.0077	[8]
$SrAlF_5$	145	0.65	0.0164	[9]
$BaZnF_4$	155	0.16	0.0242	[10]
$HfF_2(SO_4)$	165	2.5	0.058	[11]
$ZrOF_4H_2$	175	2.2	0.04	[12]
$HfOF_4H_2$	185	1.8	0.043	[12]
$KBa_3Hf_2F_{14}Cl$	192.8	0.9	0.1	[13]
$KBa_3Zr_2F_{14}Cl$	194	1	0.12	[13]
$K_3Ba_2Zr_6F_{31}$	190	0.5	0.08	[14]
Li_2CaZrF_8	191	0.36	0.05	[15]
Li_2CaHfF_8	192	0.3	0.03	[15]
$K_2BaZr_2F_{12}$	195	0.6	0.05	[16]
$K_2BaHf_2F_{12}$	196	0.35	0.04	[16]
$ZrF_2(SO_4)$	206	3.2	0.074	[11]
$CsNaTaF_7$	210	0.2	0.01	[17]
$CdF(C_6H_4NO_2)(H_2O)$	265	3.2	0.26	This work
Na_2CeF_6	275	2.1	0.022	[18]
$(H_2DpA)_2SiF_6$	374	1	0.282	[19]
$(C_3N_6H_7)_2SiF_6·H_2O$	284	0	0.152	[20]
$[C_{10}H_8NO_2]_2SiF_6·H_2O$	260	0	0.38	[21]

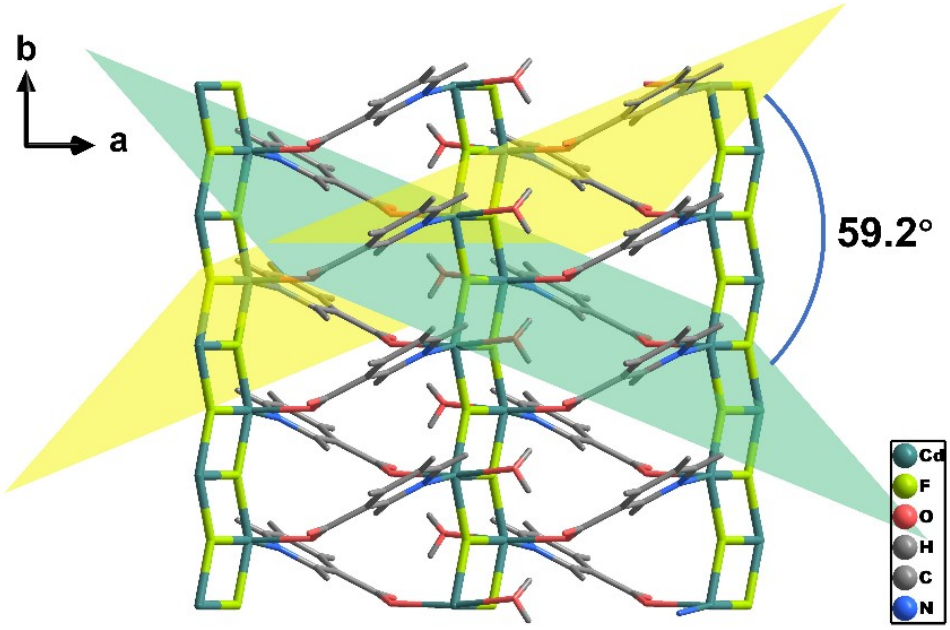

Figure S1. The angle of the organic ring in $CdF(C_6H_4NO_2)(H_2O)$.

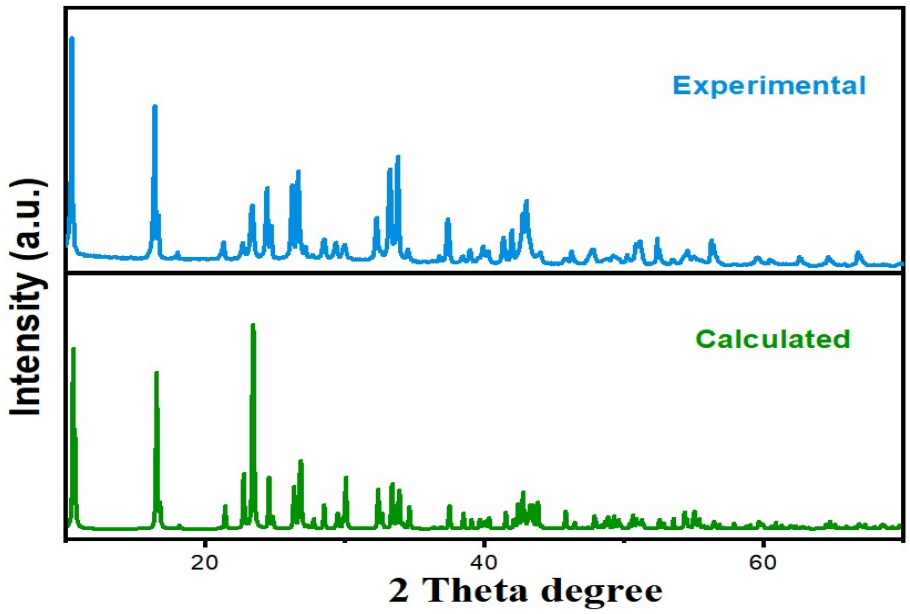

Figure S2. Calculated and experimental powder *X*-ray diffraction patterns for $CdF(C_6H_4NO_2)(H_2O)$.

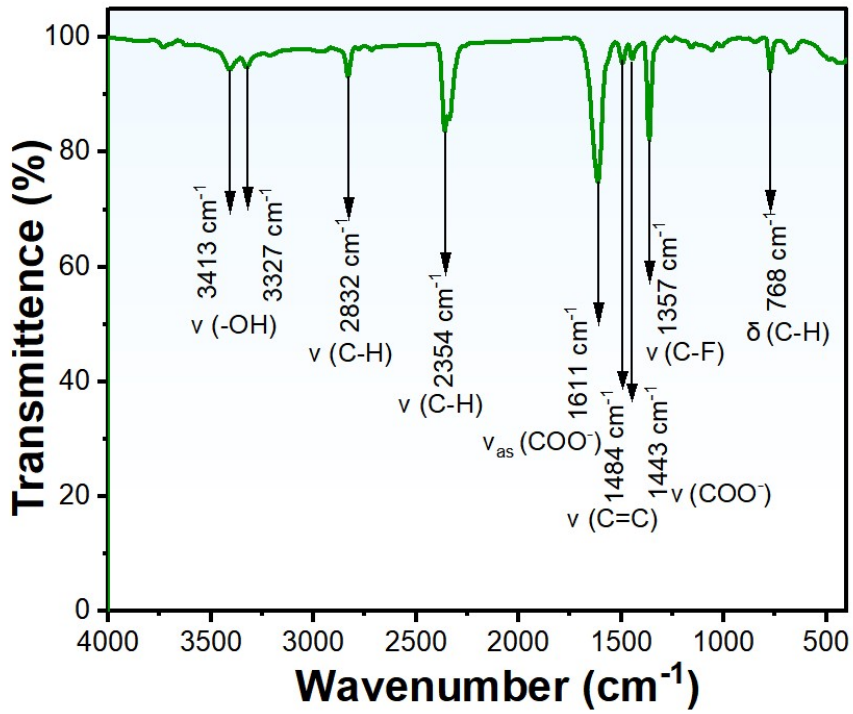

Figure S3. IR spectra for $CdF(C_6H_4NO_2)(H_2O)$.

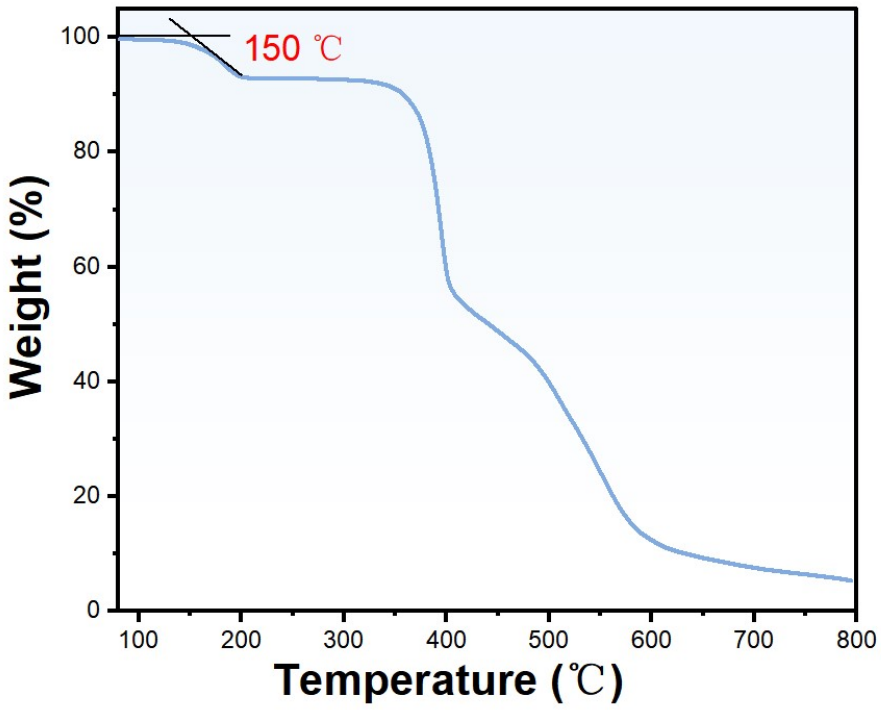

Figure S4. TG spectra for $CdF(C_6H_4NO_2)(H_2O)$.

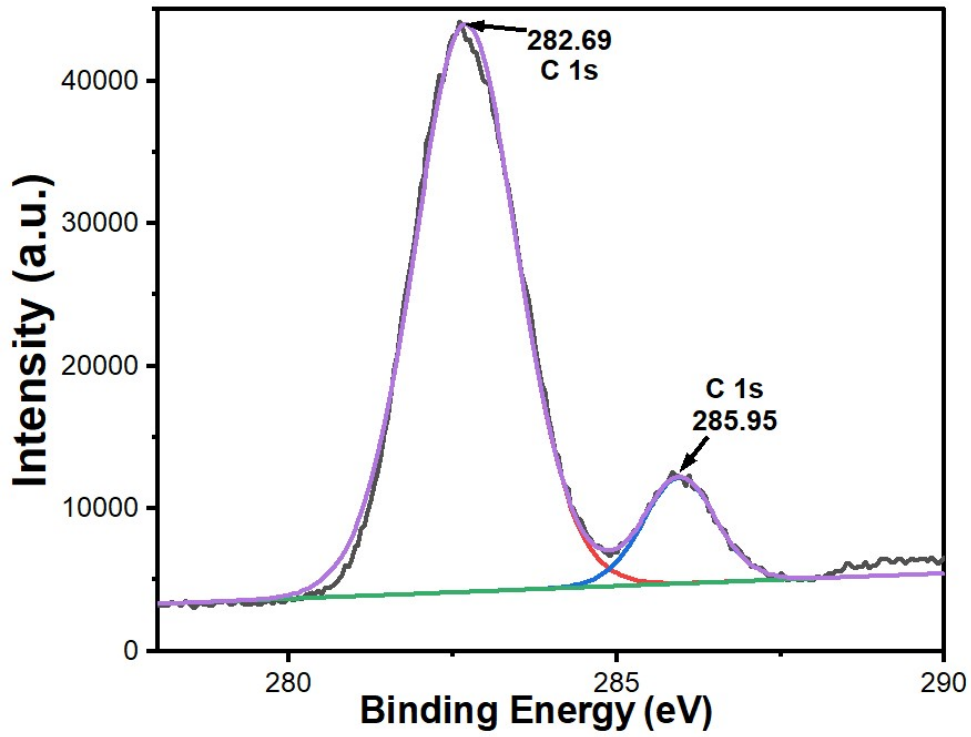

Figure S5. The XPS spectrum of the 1s orbitals of C-1s in the for $CdF(C_6H_4NO_2)(H_2O)$.

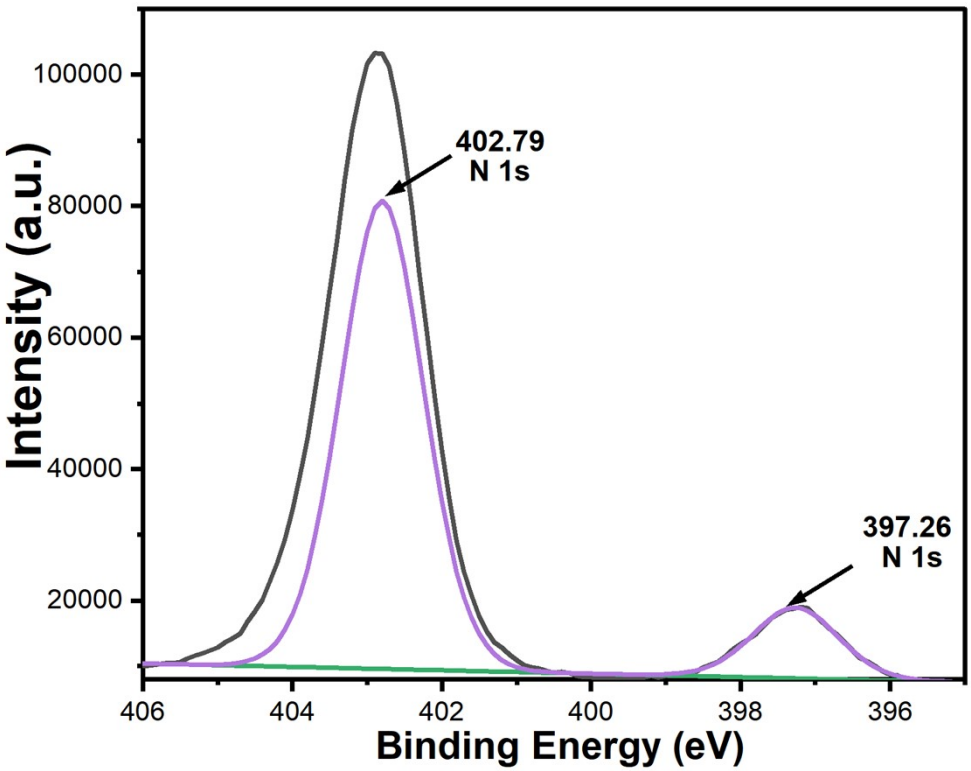

Figure S6. The XPS spectrum of the 1s orbitals of N-1s in the for $CdF(C_6H_4NO_2)(H_2O)$.

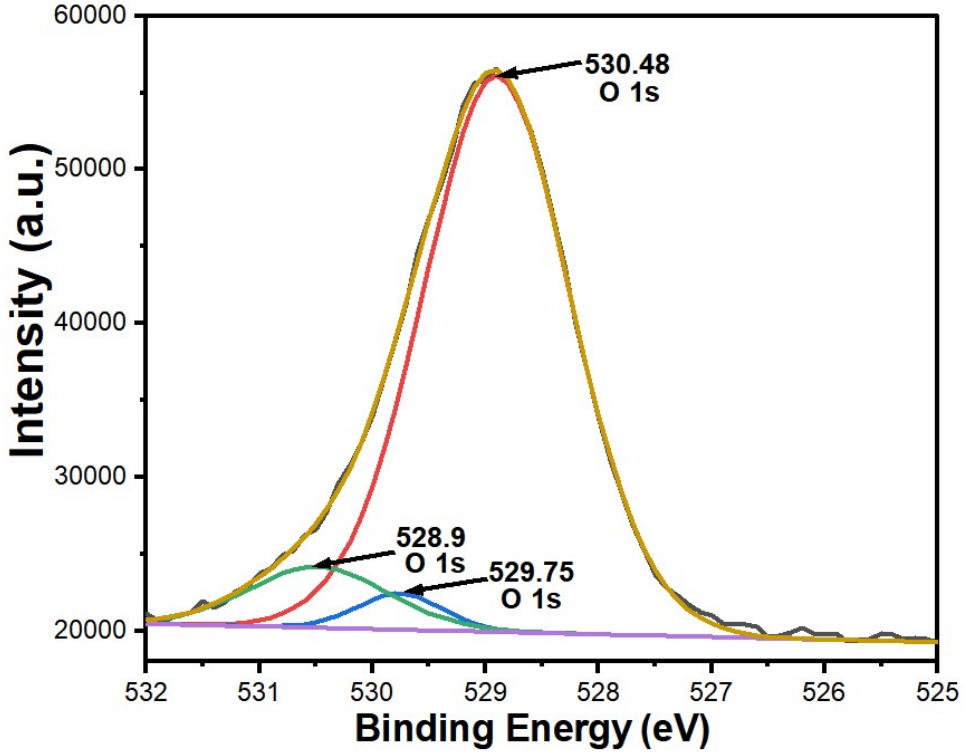

Figure S7. The XPS spectrum of the 1s orbitals of O-1s in the for $CdF(C_6H_4NO_2)(H_2O)$.

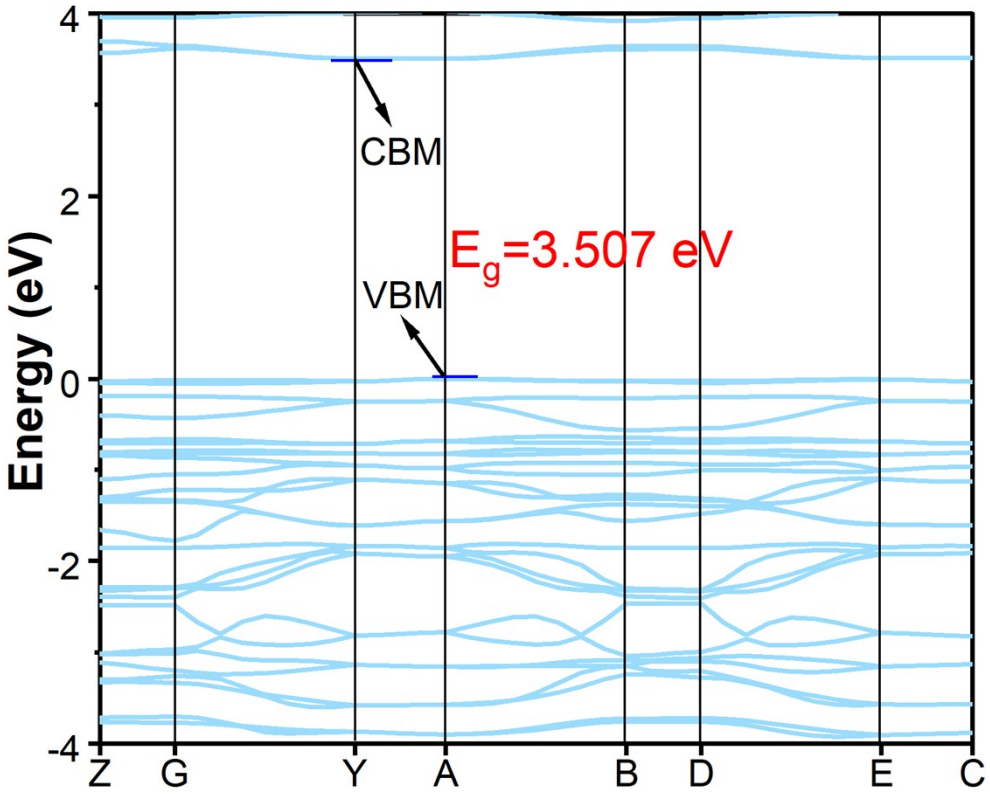

Figure S8. The calculation for the band structure of $CdF(C_6H_4NO_2)(H_2O)$.

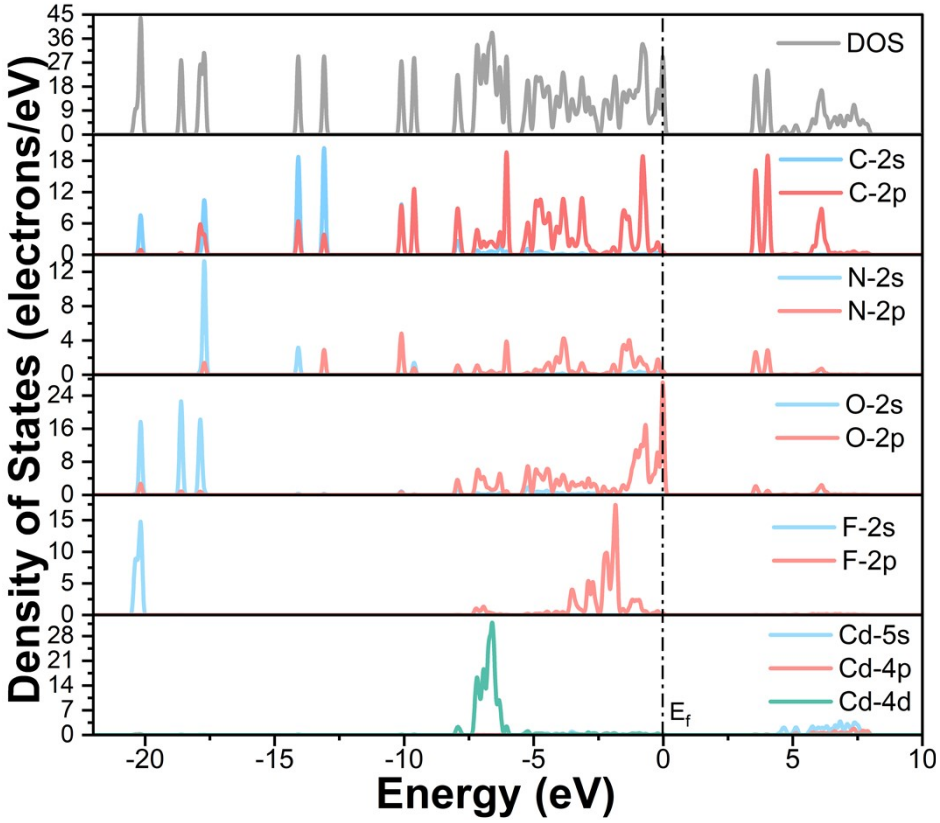

Figure S9. The calculation for the density of states of $CdF(C_6H_4NO_2)(H_2O)$.

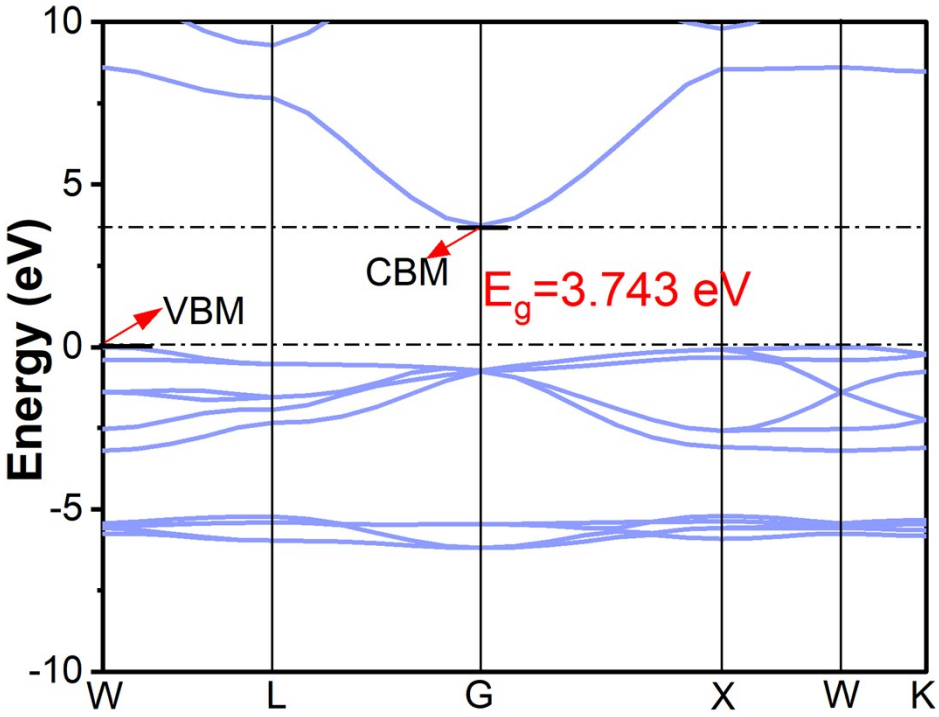

Figure S10. The calculation for the band structure of CdF_2.

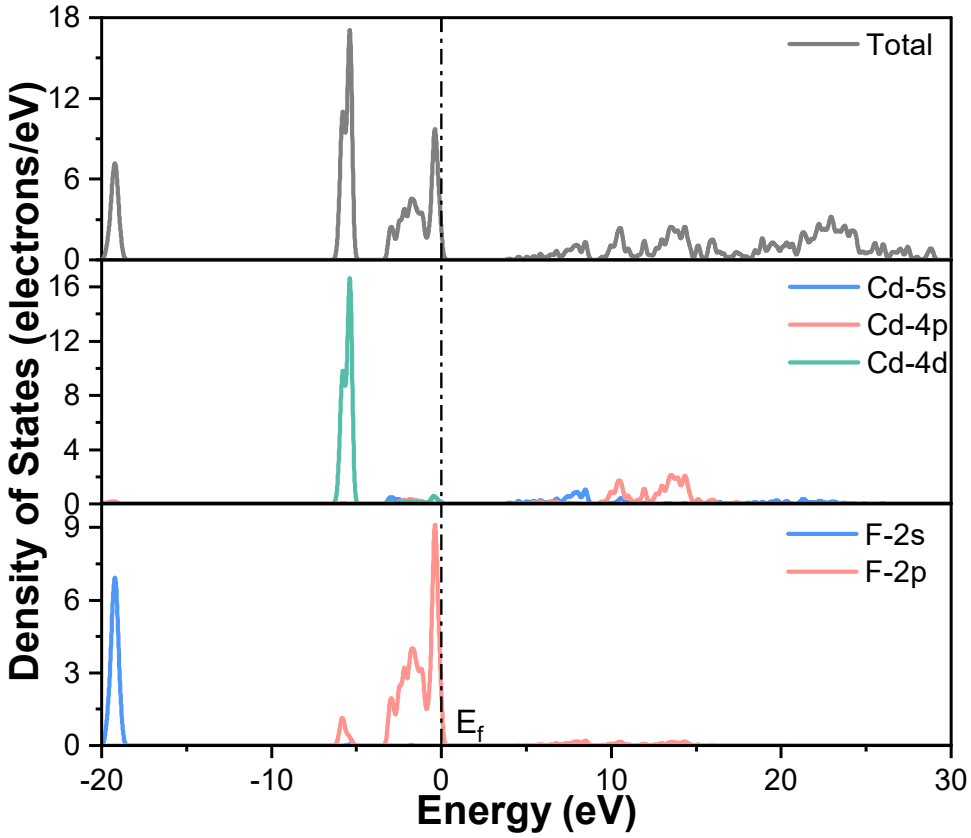

Figure S11. The calculation for the density of states of CdF_2.

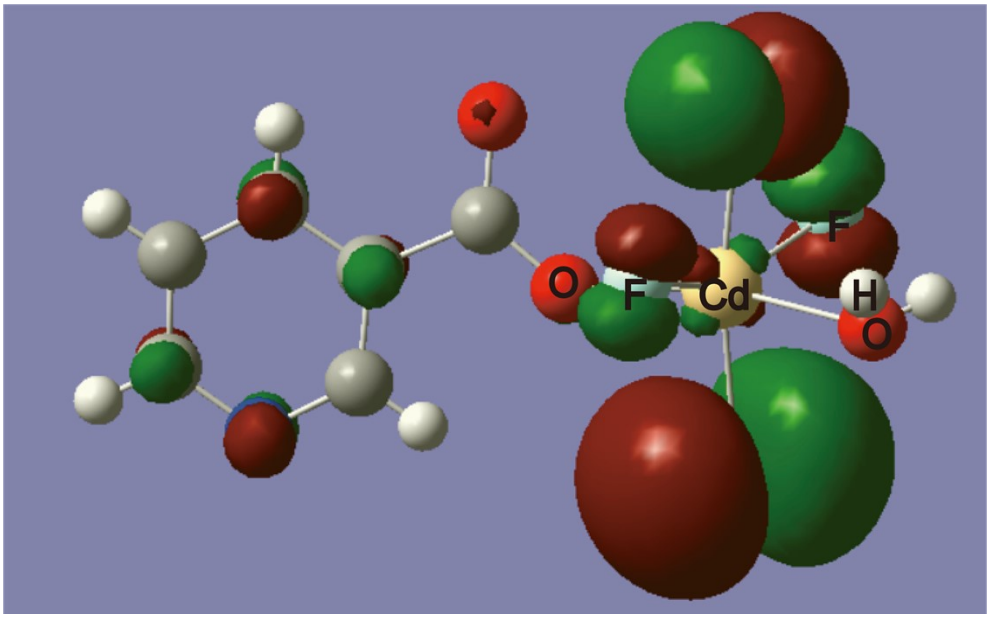

Figure S12. The calculation for the HOMO of $CdF(C_6H_4NO_2)(H_2O)$.

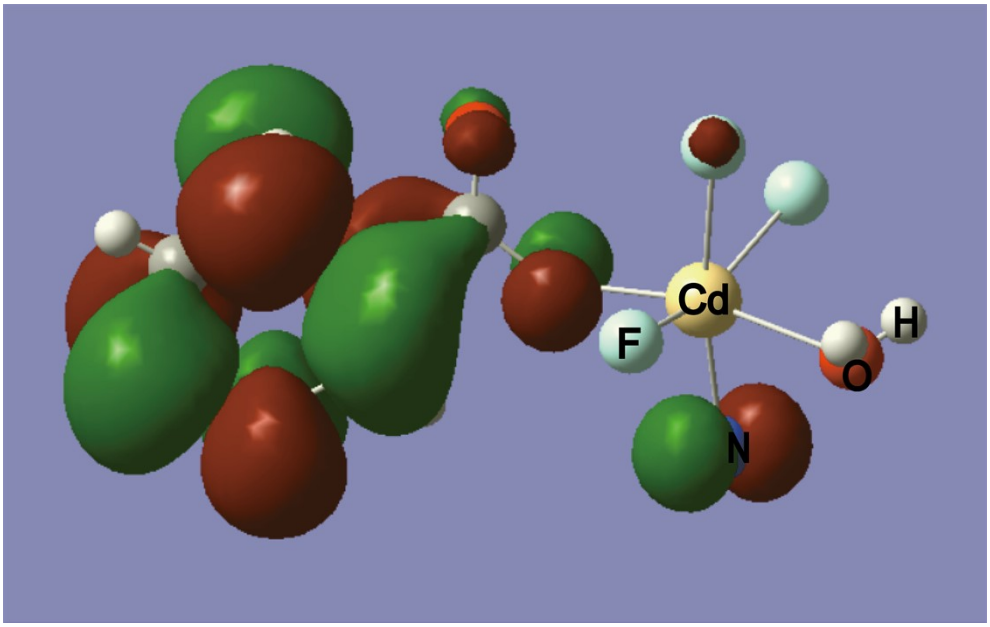

Figure S13. The calculation for the LUMO of $CdF(C_6H_4NO_2)(H_2O)$.

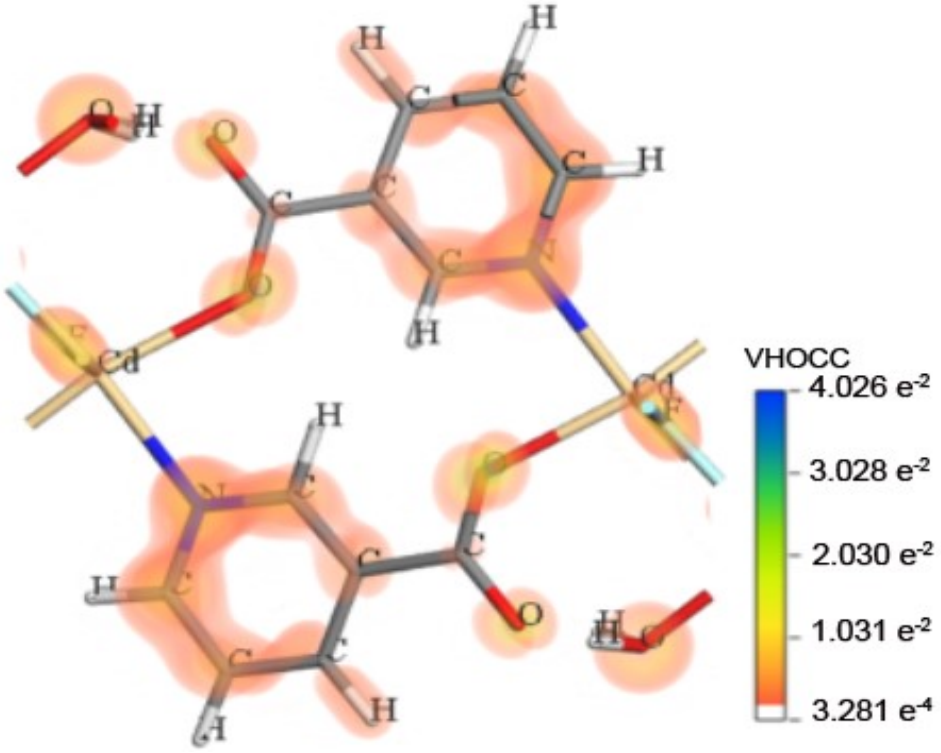

Figure S14. The calculation for the VHOCC for $CdF(C_6H_4NO_2)(H_2O)$.

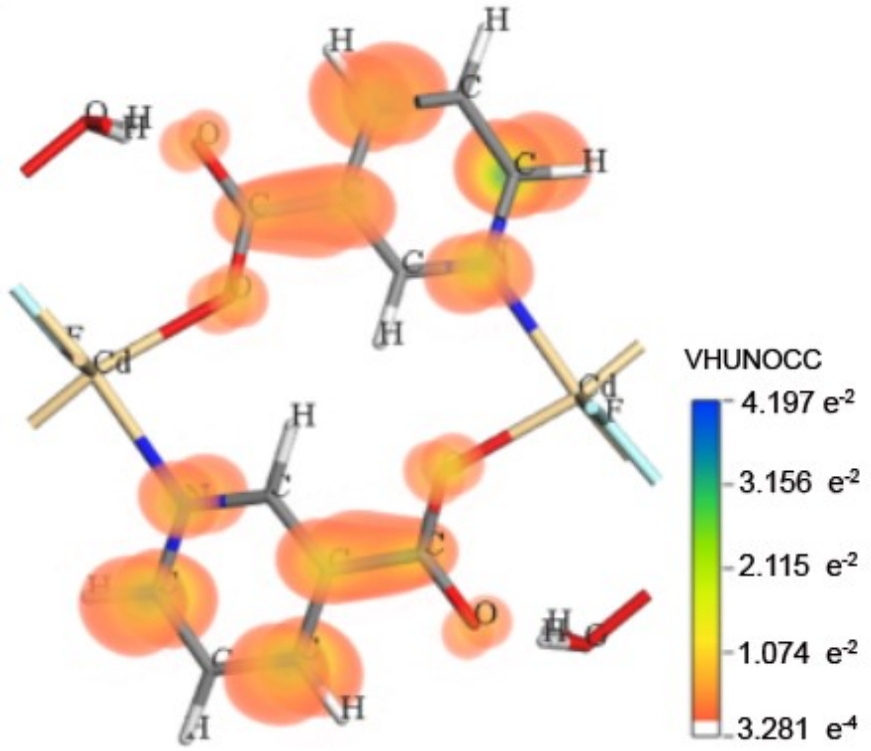

Figure S15. The calculation for the VHUNOCC for $CdF(C_6H_4NO_2)(H_2O)$.

References

1. O. V. Dolomanov, L. J. Bourhis, R. J. Gildea, J. A. K. Howard and H. Puschmann, OLEX2: a complete structure solution, refinement and analysis program, *J. Appl. Crystallogr.*, 2009, **42**, 339-341.
2. B. E. Sørensen, A revised Michel-Lévy interference colour chart based on first-principles calculations, *Eur. J. Mineral.*, 2013, **25**, 5-10.
3. V. Milman, K. Refson, S. J. Clark, C. J. Pickard, J. R. Yates, S. P. Gao, P. J. Hasnip, M. I. J. Probert, A. Perlov and M. D. Segall, Electron and vibrational spectroscopies using DFT, plane waves and pseudopotentials: CASTEP implementation, *J. Mol. Struct. THEOCHEM*, 2010, **954**, 22-35.
4. I. D. Brown, Recent developments in the methods and applications of the bond valence model, *Chem. Rev.*, 2009, **109**, 6858-6919.
5. P. Wisesa, K. A. McGill and T. Mueller, Efficient generation of generalized Monkhorst-Pack grids through the use of informatics, *Phys. Rev. B*, 2016, **93**, 155109.
6. D. J. Moss, E. Ghahramani, J. E. Sipe and H. M. Van Driel, Band-structure calculation of dispersion and anisotropy in χ→(3) for third-harmonic generation in Si, Ge, and GaAs, *Phys. Rev. B*, 1990, **41**, 1542.
7. W. Cheng, C. Lin, H. Zhang and G. Chai, Theoretical evaluation on terahertz source generators from ternary metal chalcogenides of PbM_6Te_{10} (M= Ga, In), *J. Phys. Chem. C*, 2018, **122**, 4557-4564.
8. L. Mateos, M. O. Ramírez, I. Carrasco, P. Molina, J. F. GalisteoLópez, E. G. Víllora, C. de las Heras, K. Shimamura, C. Lopez and L. E. Bausá, $BaMgF_4$: An Ultra-Transparent Two-Dimensional Nonlinear Photonic Crystal with Strong χ (3) Response in the UV Spectral Region, *Adv. Funct. Mater.*, 2014, **24**, 1509-1518.
9. E. G. Víllora, K. Shimamura, K. Muramatsu, S. Takekawa, K. Kitamura and N. Ichinose, Refractive index of $SrAlF_5$ and derived grating period for UV/VUV quasi-phase-matching SHG, *J. Cryst. Growth*, 2005, **280**, 145-150.

10. J. G. Bergman, G. R. Crane and H. Guggenheim, Linear and nonlinear optical properties of ferroelectric $BaMgF_4$ and $BaZnF_4$, *J. Appl. Phys.*, 1975, **46**, 4645-4646.
11. C. Wu, C. Jiang, G. Wei, X. Jiang, Z. Wang, Z. Lin, Z. Huang, M. G. Humphrey and C. Zhang, Toward large second-harmonic generation and deep-UV transparency in strongly electropositive transition metal sulfates, *J. Am. Chem. Soc.*, 2023, **145**, 3040-3046.
12. C. Jiang, X. Jiang, C. Wu, Z. Huang, Z. Lin, M. G. Humphrey and C. Zhang, Isoreticular design of $KTiOPO_4$-like deep-ultraviolet transparent materials exhibiting strong second-harmonic generation, *J. Am. Chem. Soc.*, 2022, **144**, 20394-20399.
13. MeiYan, L. Chun, L. Ru, D. Wen, WenlongLiu and P. Sheng, $KBa_3M_2F_{14}Cl$ (M = Zr, Hf): novel short-wavelength mixed metal halides with the largest second-harmonic generation responses contributed by mixed functional moieties, *Chem. Sci.*, 2024, **15**, 8500-8505.
14. M. Yan, R. Tang, W. Yao, W. Liu and S. Guo, Exploring a new short-wavelength nonlinear optical fluoride material featuring unprecedented polar cis-$[Zr_6F_{34}]^{10-}$ clusters, *Chem. Sci.*, 2024, **15**, 2883-2888.
15. M. Yan, R. Tang, W. Xu, W. Liu and S. Guo, Centrosymmetric $CaBaMF_8$ and Noncentrosymmetric Li_2CaMF_8 (M = Zr, Hf): Dimension Variation and Nonlinear Optical Activity Resulting from an Isovalent Cation Substitution-Oriented Design, *Inorg. Chem.*, 2024, **63**, 5260-5268.
16. M. Yan, R. L. Tang, W. D. Yao, W. Liu and S. P. Guo, From $CaBaM_2F_{12}$ to $K_2BaM_2F_{12}$ (M = Zr, Hf): Heterovalent Cation-Substitution-Induced Symmetry Break and Nonlinear-Optical Activity, *Inorg. Chem.*, 2024, **12**.
17. R. L. Tang, X. Lian, X. Li, L. Huai, W. Liu and S. P. Guo, From $CsKTaF_7$ to $CsNaTaF_7$: Alkali Metal Cations Regulation to Generate SHG Activity, *Chem. Eur. J.*, 2022, **28**, e202201588.
18. R. Tang, W. Xu, X. Lian, Y. Wei, Y. L. Lv, W. Liu and S. Guo, Na_2CeF_6: A Highly Laser Damage-Tolerant Double Perovskite Type Ce (IV) Fluoride Exhibiting Strong Second-Harmonic Generation Effect, *Small*, 2024, **20**, 2308348.
19. Q. Y. Chen, A hydrogen-bonded inorganic-organic network with noncentrosymmetric structure exhibiting second-order nonlinear optical response, *Inorg. Chem. Commun.*, 2018, **98**, 150-153.
20. Shen Y, Chen B, Chen H, et al. $(C_3N_6H_7)_2SbF_5{\cdot}H_2O$ exhibiting strong optical anisotropy from the optimal arrangement of π-conjugated $(C_3N_6H_7)^+$ groups, *Inorg. Chem.*, 2022, **61**, 14242-14246.
21. Liu L, Huang H, Ding M, et al. Noncentrosymmetric Crystal $[C_{10}H_8NO_2]_2SiF_6{\cdot}H_2O$ with LargeBirefringence, *Inorg. Chem.*, 2024, **63**, 13835-13839.